TRENDS IN SCIENCES 2026; 23(12): 12778
https://doi.org/10.48048/tis.2026.12778 RESEARCH ARTICLE

Caffeic Acid Derivatives as Promising Efflux Pump Inhibitors Against Multidrug-Resistant *Pseudomonas aeruginosa*: Insights from Molecular Docking Studies

Noor Zawani Zakaria[1], Habibah A Wahab[1], Suriani Mohamad[1] and Ezatul Ezleen Kamarulzaman[2,3,4,*]

[1]Department of Pharmaceutical Technology, School of Pharmaceutical Sciences, Universiti Sains Malaysia, Pulau Pinang 11800, Malaysia
[2]Department of Pharmaceutical Chemistry, School of Pharmaceutical Sciences, Universiti Sains Malaysia, Pulau Pinang 11800, Malaysia
[3]Faculty of Pharmacy, Universitas Airlangga, Kampus C UNAIR, Jl. Mulyorejo, Mulyorejo, Surabaya, East Java 60115, Indonesia
[4]Faculty of Pharmacy, Universitas Hasanuddin, Jl. Perintis Kemerdekaan No.KM 10, Tamalanrea Indah, Kec. Tamalanrea, Kota Makassar, Sulawesi Selatan 90245, Indonesia

([*]Corresponding author's e-mail: ezatulezleen@usm.my)

Received: 24 November 2025, Revised: 3 March 2026, Accepted: 15 March 2026, Published: 10 July 2026

Abstract

Pseudomonas aeruginosa is a highly resilient bacterial pathogen intrinsically resistant to multiple antibiotics due to its low outer membrane permeability and the overexpression of multidrug efflux pumps, particularly MexAB-OprM. Targeting efflux activity through efflux pumps inhibitors (EPIs) represents a promising strategy to restore antibiotic efficacy. This *in silico* study explores caffeic acid and its structurally diverse derivatives (benzyl caffeate, caffeoylmalic acid, caftaric acid, caffeic acid phenethyl amide (CAPA), caffeic acid phenethyl ester (CAPE), dihydrocaffeic acid, ethyl caffeate, methyl caffeate, octyl caffeate, prenyl caffeate, and rosmarinic acid) as potential EPIs targeting *P. aeruginosa*, specifically the MexB protein of the MexAB-OprM system. Molecular docking simulations were performed using AutoDock 4.2 to determine binding affinities and interaction profiles of the selected compounds within the MexB distal binding pocket. Docking analysis revealed that all derivatives preferentially localized to the distal binding pocket of the MexB transporter, interacting extensively with hydrophobic and aromatic residues enriched in the PN2 and PC1 subdomains of the T monomer. These regions are enriched with phenylalanine residues (Phe136, Phe178, Phe610, Phe615 and Phe628), which facilitate with π–π stacking and hydrophobic interactions and hydrogen bond interaction. Among the tested compounds, CAPE and CAPA showed the most favorable docking energies and interaction patterns, with binding conformations closely mimicking the binding behavior of those established EPI, ABI-PP. Although their binding energies were moderately higher than ABI-PP, CAPA and CAPE demonstrated strong structural alignment and interaction with key residues, suggesting their potential as novel efflux pump inhibitors to combat multidrug resistance in *P. aeruginosa*. Overall, these findings suggest that CAPA and CAPE possess promising structural features for efflux pump inhibition and may serve as lead compounds for the development of novel adjuvant therapies against multidrug-resistant *P. aeruginosa*. Further experimental validation is warranted to confirm their inhibitory potential and assess their clinical relevance.

Keywords: Multidrug resistance, *Pseudomonas aeruginosa*, Mex B protein, Efflux pump inhibitor, Caffeic acid derivatives, Molecular docking, AutoDock

Introduction

Pseudomonas aeruginosa is a Gram-negative opportunistic human pathogen renowned for its remarkable adaptability and ability to survive in diverse environmental niches [1]. It is also a leading cause of nosocomial infections worldwide [2]. Individuals with compromised immune systems such as those with cystic fibrosis, cancer, or diabetes and patients suffering from burns or severe trauma are particularly vulnerable to infections caused by *P. aeruginosa* [3,4]. Over the years, *P. aeruginosa* has developed significant resistance to a broad range of antimicrobials, earning it the classification of a 'superbug'. Its intrinsic multidrug resistance is primarily attributed to the expression of efflux pumps belonging to the resistance-nodulation-division (RND) superfamily [5,6].

The MexAB-OprM system is the most constitutively expressed and clinically relevant of this RND family, with MexB serving as the inner membrane transporter responsible for substrate recognition and energy-dependent efflux [7,8]. These efflux pumps actively extrude antibiotics from the bacterial cell, reducing intracellular drug accumulation and thereby diminishing antibiotic efficacy. MexB recognizes and transports a broad spectrum of antibiotics, including B-lactams, fluoroquinolones, tetracyclines, chloramphenicol and macrolides [7]. MexB is frequently overexpressed in multidrug-resistant (MDR) and extensively drug-resistant (XDR) clinical isolates of *P. aeruginosa*. Its activity significantly reduces the intracellular concentration of antibiotics, rendering many treatments ineffective. Inhibiting MexB has been shown to restore antibiotic susceptibility *in vitro*, making it a promising target for efflux pump inhibitors (EPIs) [9].

Efflux pump inhibitors (EPIs) represent a promising strategy to restore antibiotic activity by preventing the active export of antimicrobials. EPIs are small molecules that act as adjuvants to conventional antibiotics, functioning through either competitive or non-competitive-inhibition of efflux pump activity [10]. By blocking efflux activity, EPIs can enhance the intracellular concentration of antibiotics, thereby increase their potency and potentially slow the emergence of resistant bacterial strains [8]. Among the most studied EPIs is phenyl-arginine β-naphthylamide (PAβN), which was the first broad-spectrum inhibitor known to target all 4 major RND efflux systems in *P. aeruginosa*, as well as in other Gram-negative bacteria [11-13]. However, despite its broad activity, PAβN has not advanced to clinical use due to poor pharmacokinetic properties, toxicity concerns, and its disruptive effects on bacterial membrane integrity [12,13].

For centuries, medicinal plants have served as rich sources of therapeutic agents used to treat bacterial, fungal, and viral infections [14]. Their pharmacological potential is largely attributed to the abundance of structurally diverse phytochemicals, which possess a wide array of bioactive properties, including antimicrobial activity [15]. Caffeic acid (CA), also known as 3,4-dihydroxycinnamic acid, is a polyphenolic organic acid [16-20]. It is ubiquitously distributed in plant tissues and is prevalent in diverse sources, including coffee, vegetables, fruits, olive oil, cereals, as well as medicinal plants such as rosemary *(Rosmarinus officinalis),* sage *(Salvia officinalis),* thyme *(Thymus vulgaris),* spearmint *(Mentha spicata),* balm *(Melissa officinalis),* and lavender *(Lavandula spp.)* [16,17,21-25]. Beyond natural occurrence, caffeic acid and its derivatives including esters, amides, and hybrid conjugates can also be obtained through chemical synthesis [26-31] or produced via metabolic pathways [32], providing access to compounds with desirable attributes. In the context of the present *in silico* study, the origin (natural vs synthetic) of CA derivatives is not determinative, as molecular docking evaluates ligand-protein interactions based on chemical structure rather than source. Caffeic acid and its related compounds such as chlorogenic acid and caffeic acid phenethyl ester (CAPE) are well known for their broad pharmacological profiles, including antibacterial, antifungal, antiviral, antioxidant, and anticancer activities [25,27,28, 33-41]. Given this pharmacological profile and their physicochemical suitability for engaging hydrophobic and aromatic residues within efflux transporters, CA derivatives were selected as rational candidates for investigating potential inhibition of the MexB component of the MexAB-OprM system.

In view of the growing interest in plant-derived compounds as potential antibiotic adjuvants, this study aims to identify the binding interaction of the novel efflux pump inhibitor (EPI) candidates derived from

caffeic acid and its structural analogues as a potential strategy to counteract multidrug resistance (MDR) in *P. aeruginosa*. Candidate caffeic acid derivatives for this study were selected based on reported biological activities and structural diversity, with particular emphasis on variations in atomic composition and functional group characteristics. To evaluate the potential these caffeic acid derivatives as EPI candidates, *in silico* molecular docking simulations will be employed to assess the binding affinities and interaction profiles of these derivatives with the *P. aeruginosa* efflux pump Mex B protein.

Materials and methods

In silico prediction of caffeic acid derivatives interaction with MexB efflux pump protein in *P. aeruginosa*

The interactions and binding affinities of the selected caffeic acid derivatives toward the efflux pump protein, MexB, were predicted using a molecular docking technique. Docking simulations were carried out using AutoDockTools 1.5.6 (ADT) and AutoDock 4.2 software (The Scripps Research Institute, USA; www.autodock.scripps.edu), with the ligands modeled as flexible entities. The docking procedure followed the established AutoDock 4.2 protocol described by Morris *et al.* [42], comprising 4 key stages: (i) preparation of the rigid target protein structures (MexB), with all heteroatoms and solvent molecules removed; (ii) construction and optimization of ligand structures; (iii) generation of atomic grid maps for each ligand atom type using AutoGrid; and (iv) execution of the docking simulations employing the Lamarckian Genetic Algorithm (LGA) to predict optimal ligand-protein binding conformations and estimate binding energies.

Preparation of target macromolecules and binding site identification

At the time this study was carried out, the crystal structure of the MexB transporter from the MexAB-OprM efflux system in *Pseudomonas aeruginosa* was retrieved from the RCSB Protein Data Bank (PDB ID: 3W9J; https://www.rcsb.org/structure/3W9J), resolved at a 3.15 Å resolution and used as the structural template for docking analyses. This structure contains a co-crystallized efflux pump inhibitor (EPI), a pyridopyrimidine derivative known as ABI-PP, chemically described as [{2-[({[(3R)-1-{8-[(4-tert-butyl-1,3-thiazol-2-yl)carbamoyl]-4-oxo-3-[(E)-2-(1H-tetrazol-5-yl)ethenyl]-4H-pyrido[1,2-a]pyrimidin-2-yl}piperidin-3-yl)oxy}carbonyl)amino]ethyl}(dimethyl) ammonio] acetate. For molecular docking studies, chain B of the MexB trimer specifically the monomer bound to ABI-PP was selected in this study (**Figure 1**).

Prior to docking, all non-essential elements including water molecules, ions, and co-crystallized ligands were removed from the PDB file. Hydrogen atoms were added, and atomic charges were assigned using the Kollmann charges. The prepared protein monomer was then saved in PDBQT format for subsequent molecular docking analysis. The active site of MexB was defined based on the binding pocket of ABI-PP, comprising key residues previously identified to interact with the inhibitor: Phe136, Lys151, Phe178, Asp274, Phe573, Phe610, Phe615, Arg620, and Phe628 [43].



Figure 1 Three-dimensional structures of MexB protein. Chain B (tight / binding conformation) of MexB protein co-crystallized with ABI-PP (colored as yellow in space-fill formatting) retrieved from PDB (Code: 3W9J. This figure was generated using Discovery Studio 4.1 Visualizer program.

Ligand preparation

Before proceeding with docking simulations, the caffeic acid derivatives were pre-screened for drug-likeness using Lipinski's Rule of Five [44], implemented via the Raccoon2 interface [45]. Compounds exceeding the threshold criteria, i.e., more than 5 hydrogen bond donors, more than 10 hydrogen bond acceptors, a molecular weight greater than 500 Da, or a calculated logP exceeding 5 were excluded from further analysis. Twelve compounds, as depicted in **Figure 2**, satisfied all Lipinski's criteria and were thus selected as ligands for molecular docking simulation with MexB.

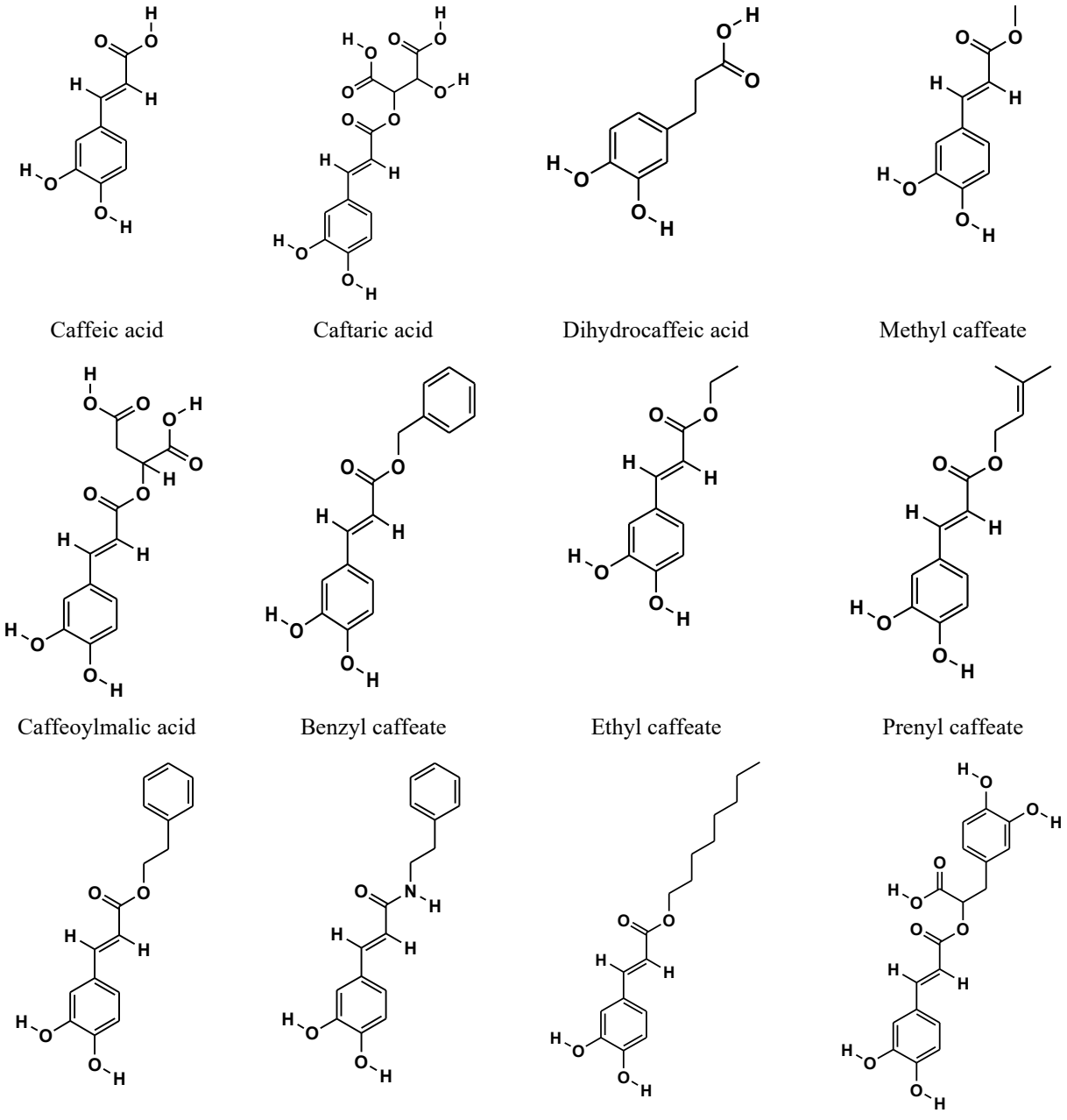


Figure 2 Chemical structure of the caffeic acid derivatives used in this study.

Positive control data set validation

The validation of the docking protocol was carried by redocking the extracted co-crystallized ligand ABI-PP into the binding pocket of the MexB protein as a positive control. The initial 3-dimensional structure of ABI-PP was obtained from the Protein Data Bank (PDB ID: 3W9J). The partial atomic charges were automatically assigned using the Gasteiger charges within AutoDockTools (ADT). The optimal torsion tree root was determined, and rotatable bonds were automatically assigned in ADT. The prepared ligand structure was subsequently saved in the PDBQT format required for AutoDock 4.2.

Preparation of test compounds

The chemical structures of the selected caffeic acid derivatives were retrieved from previously published literature. The chemical structures of each ligand were built by initially constructing the 2D structure using ChemBioDraw CambridgeSoft Corporation, PerkinElmer, Inc. (www.cambridgesoft.com). All bonds were modified appropriately, and all missing hydrogen atoms were added to satisfy their reported structures. The 2D structures were then converted into 3-dimensional (3D) models and subjected to energy minimization using the MM2 force field in Chem3D Pro with default parameters. The optimized structures were saved in PDB format. Subsequently, all ligand structures underwent standard preparation in AutoDockTools. Gasteiger partial charges were assigned, torsion tree roots were defined, and rotatable bonds were automatically set. The fully prepared ligands were then exported in PDBQT format for molecular docking analysis using AutoDock 4.2.

Grid map calculation

The grid map calculations were done using AutoGrid from ADT. The grid map was set at x = 33.942, y = 17.207 and z = −57.587, which is at the centre axis of the crystal structure coordinates of ABI-PP in the complex of MexB with dimension of 40 Å x 40 Å x 58 Å in x, y and z axes. The spacing between grid points (distance between each probe atom) was set to the default value of 0.375 Å and the file was then saved as gpf file.

Docking simulation

Docking simulations were executed using AutoDock 4.2, employing Lamarckian Genetic Algorithm (LGA) combined with the pseudo-Solis and Wets local search method [46,47]. Simulations for MexB were performed under consistent conditions using default parameters: (population size = 150; maximum number of evals = 2,500,000; maximum number of generations = 27,000, maximum number of top individuals that automatically survive = 1, rate of gene mutation = 0.02 and rate of crossover = 0.8) and a total of 100 genetic algorithm (GA) runs were carried out in this docking process. Upon completion of the docking simulations, the results were ranked based on the lowest binding free energy, predicted inhibition constant (Ki), and protein-ligand interaction profiles. Protein-ligand interactions were visualized and analyzed using Discovery Studio Visualizer 4.1 (Accelrys Software Inc., USA) and validated through LigPlot v1.4.5 [48] for detailed interaction mapping.

Results and discussion

Computational docking of caffeic acid derivatives against MexB

Following an evaluation based on Lipinski's Rule of Five, all 12 caffeic acid derivatives were found to comply with the rule and were subsequently selected for protein-ligand interaction studies with the MexB efflux pump using AutoDock 4.2 (**Table 1**). These compounds included caffeic acid, benzyl caffeate, caffeoylmalic acid, caftaric acid, caffeic acid pheneythyl amide (CAPA), caffeic acid pheneythyl ester (CAPE), dihydrocaffeic acid, ethyl caffeate, methyl caffeate, octyl caffeate, prenyl caffeate, and rosmarinic acid. In this study, the selected caffeic acid derivatives share a common structural feature, an aromatic catechol unit (2-hydroxyphenyl group), which acts as a crucial pharmacophore within this compound class. Additionally, several derivatives contain ionizable functional groups, such as carboxylic acids or amides, that can influence their physicochemical characteristics, including solubility and ionization behavior under physiological conditions [30,49,50]. The presence of aromatic and hydrophobic groups in these compounds is expected to facilitate hydrogen bond interactions as well as non-covalent interactions within the hydrophobic

binding pocket of MexB, including π–π stacking, hydrophobic contacts, and van der Waals forces [51].

Structural variations among the compounds, such as differences in alkyl chain length and functional group substitution, were expected to influence their potential as EPIs. For instance, CAPE and CAPA differ by an ester-to-amide substitution, a modification that may affect molecular stability and binding affinity towards efflux pump [52]. These structural features contribute to the amphiphilic nature of the compounds, which is an important attribute since RND-type efflux transporters preferentially recognize and target amphiphilic substrates, including many antibiotics [53].

Table 1 Molecular properties and drug-likeness of selected caffeic acid derivatives.

Compounds	PubChem CID	Molecular Weight (g/mol)	Log P (Octanol-Water partition coefficient value)	H-Bond Donor	H-Bond Acceptor
Caffeic acid	689043	180.2	1.2	3	4
Caftaric acid	6440397	312.2	0.1	5	9
CAPE	5281787	284.3	4.2	2	4
CAPA	11391937	283.3	2.7	3	3
Caffeoylmalic acid	6124299	296.2	0.6	4	8
Dihydrocaffeic acid	348154	182.2	-0.5	3	4
Benzyl caffeate	5919576	270.3	3.1	2	4
Ethyl caffeate	5317238	208.2	2.6	2	4
Prenyl caffeate	5281790	248.27	3.0	2	4
Octyl caffeate	10108392	292.4	5.7	2	4
Methyl caffeate	689075	194.2	1.5	2	4
Rosmarinic acid	5281792	360.3	2.4	5	8

In addition to their favorable drug-like properties supported by Lipinski's Rule of Five, the selection of caffeic acid and its derivatives is reinforced by substantial experimental evidence demonstrating their antimicrobial and antioxidant activities. Caffeic acid derivatives commonly categorized into ester, amide, and hybrid conjugates have shown notable *in vitro* potency across multiple bioassays [30,31]. For example, several ester derivatives exhibit antifungal activity against *Candida albicans*, with MIC_{50} values as low as 13 μM (e.g., CAP10) and 32 μg/mL (e.g., compound 1g). Strong antioxidant activities have also been reported, with compounds such as 3k, 5a, CS2, Phellinsin A, and 8j displaying DPPH radical-scavenging IC_{50} values of 18.6 μM, 67.85 μM, 40.29 μM, 0.29 ± 0.004 mM, and 4,774.37 ± 137.20 μM, respectively [30,31]. Collectively, these findings highlight the biological relevance of caffeic acid-based scaffolds and provide a solid experimental foundation for their evaluation as potential efflux pump inhibitors in molecular docking studies targeting the MexB transporter.

Using the crystal structure of MexB protein (PDB code: 3W9J), resolved at 3.15 Å [43]. MexB is the integral membrane protein of the MexAB-OprM efflux system in *P. aeruginosa* and is responsible for the recognition and binding of a broad range of antimicrobial agents and other drugs/ligands [43]. Besides displaying a good structural resolution, the availability of a holo (ligand-bound) structure is an important criterion to be considered in target protein selection for structure-based drug design [54]. Although other MexB crystal structures with a better (higher) resolution, such as the detergent-bound MexB crystal structures (PDB code: 3W9I; resolution 2.71 Å, and PDB code: 2V50; resolution 3.00 Å) are available, the MexB protein (3W9J) was chosen because it represents

the first EPI-bound crystal structure of MexB protein available at the time the docking was conducted.

This MexB protein was co-crystallized to an established EPI, a pyridopyrimidine derivative: [{2-[({[(3R)-1-{8-[(4-tert-butyl-1,3-thiazol-2-yl)carbamoyl]-4-oxo-3-[(E)-2-(1H-tetrazol-5-yl)ethenyl]-4H-pyrido[1,2-a]pyrimidin-2-yl}piperidin-3-yl)oxy}carbonyl)amino]ethyl}(dimethyl)ammonio] acetate, commonly referred to as ABI-PP. The inhibitor is located in the distal binding pocket of the T (tight/binding) monomers (chains B and E) of the MexB protein. The binding pockets proposed in this T monomer are structurally configured in such a way that they may accommodate and tightly bind to ligands [55]. This is because the asymmetric unit is made up of 2 structurally identical trimers (chains ABC and DEF), all docking simulations were performed only on chain B of MexB protein. It is fortuitous that the availability of this co-crystallized structure has supplied valuable information on the protein's active site for EPI binding region, thereby allowing protocol validation by positive control docking with the bound inhibitor take place.

The computational docking of the caffeic acid derivatives was initiated by re-docking the positive control, an established inhibitor, ABI-PP into the MexB protein (PDB code: 3W9J). The docked conformation of ABI-PP was compared to its co-crystallized structure (**Figure 3(a)**), resulting in a root-mean-square deviation (RMSD) value of 1.38 Å. This low RMSD value indicates that the applied docking protocol is reliable and capable of reproducing a pose closely matching the original crystal structure. Therefore, the same validated docking parameters were subsequently employed for docking the caffeic acid derivatives with the MexB protein.

A closer inspection of the MexB ABI-PP complex is presented in **Figure 3(b)**. This figure highlights the presence of hydrophobic interactions between the tert-butyl thiazolyl aminocarboxyl pyridopyrimidine (TAP) moiety of ABI-PP and the phenylalanine cluster (Phe178, Phe610, Phe615 and Phe628), along with other residues including Val139, Ile277, Tyr327 and Val612. This implies that hydrophobic interactions play a key role in stabilizing the binding of this EPI. In addition to the formation of many hydrophobic interactions, **Figure 3(b)** also depicts the presence of a hydrogen bond between the hydroxyl group of ABI-PP and the side chain of Lys151.

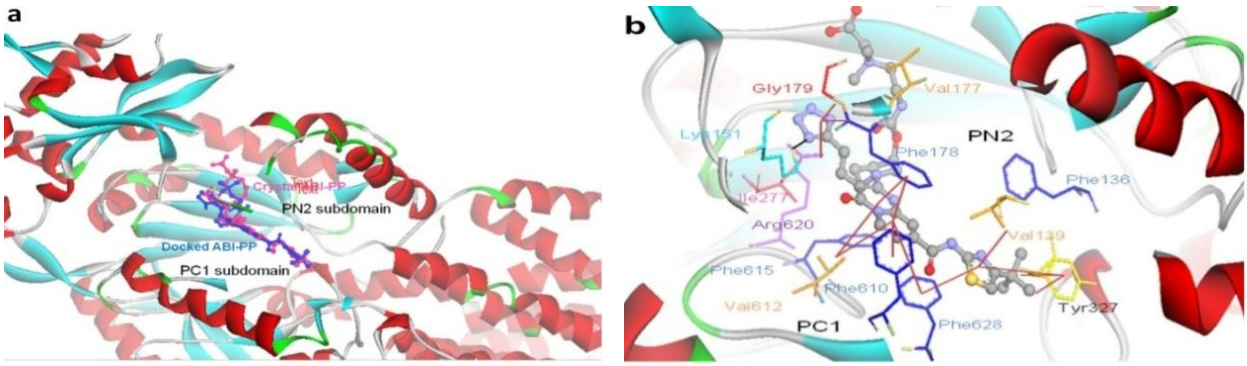


Figure 3 The graphical representation of the MexB ABI-PP complex; (a) Three-dimensional illustration of ABI-PP docked between the PC1 and PN2 subdomains of MexB. (b) Focused view of the binding site, MexB is presented as ribbon, the subdomains and the specific residues involved in the binding are labeled. The binding site is presented as stick and colored as blue for Phe, orange (Val), violet (Arg), red (Gly), magenta (Ile), yellow (Tyr) and cyan (Lys). ABI-PP is rendered as scaled ball and stick and colored based on their atom type: Grey (carbon), red (oxygen) and blue (nitrogen). Hydrogen bond and hydrophobic interactions between the ABI-PP and MexB are shown as black and red lines, respectively.

Quantitative and qualitative analyses of molecular docking

The docking of the caffeic acid derivatives with the MexB protein was carried out by utilizing the same parameters setting as those used to run the positive control (ABI-PP) docking. The superimpositions of the docked ABI-PP and caffeic acid derivatives with MexB protein is shown in **Figure 4**. Most of the caffeic acid derivatives, except for ethyl caffeate, methyl caffeate and dihydrocaffeic acid, were observed to bind within the same binding site as the ABI-PP, suggesting potential interactions with the functionally significant site of the transporter.

Molecular docking analyses, including binding free energy, predicted inhibition constants (Ki), and hydrogen bond interactions, are summarized in **Table 2**. As expected, the control compound ABI-PP exhibited the strongest binding affinity towards the MexB transporter, with a binding free energy of –11.37 kcal/mol and a predicted Ki of 4.64×10^{-3} M, consistent with its well-established role as a high-affinity efflux pump inhibitor.

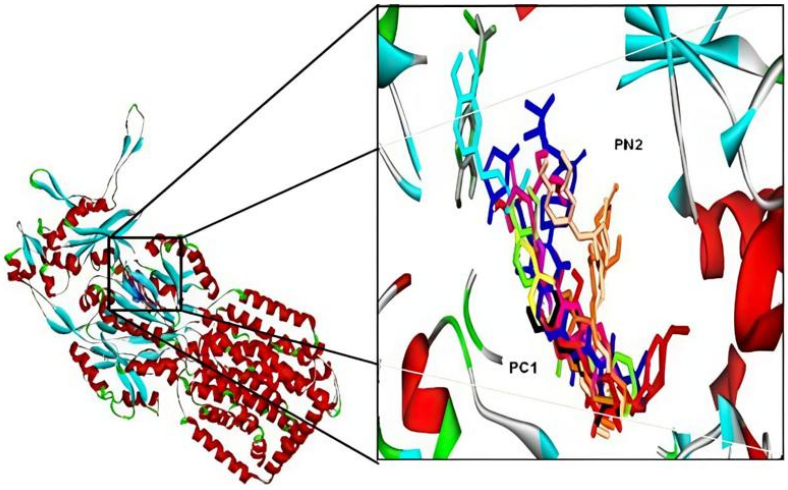


Figure 4 Ribbon representation of the docked complex of MexB with ABI-PP and the studied caffeic acid derivatives. ABI-PP and caffeic acid derivatives are rendered as stick and colored as blue for ABI-PP, violet (benzyl caffeate), yellow (caffeic acid), orange (caffeoylmalic acid), magenta (caftaric acid), red (CAPA), light green (CAPE), cyan (dihydrocaffeic acid), dark green (ethyl caffeate), black (prenyl caffeate), grey (methyl caffeate), maroon (octyl caffeate) and peach (rosmarinic acid).

Table 2 The lowest free energy of binding, ΔG, predicted inhibition constant, *K*i value and hydrogen bond interactions between ABI-PP and caffeic acid derivatives with MexB protein.

Ligands	Lowest free energy of binding, ΔG (kcal/mol)	Predicted inhibition constant, *K*i (M)	Hydrogen bond interactions		
			Total of H-bond	Ligand's atom	Amino acid residue: Atom
ABI-PP	-	-	1	N: C27	Lys151: H
ABI-PP (re-docked)	−11.37	4.64×10^{-3}	2	O: C45-OH H: C27-NH	Arg620: H Ile277: O
CAPA	−7.60	2.69	0	-	-
CAPE	−7.28	4.65	1	O: C15-OH	Lys151: H
Benzyl caffeate	−7.17	5.58	1	O: C6-OH	Lys151: H
Octyl caffeate	−6.83	9.80	0	-	-

Ligands	Lowest free energy of binding, ΔG (kcal/mol)	Predicted inhibition constant, *K*i (M)	Hydrogen bond interactions		
			Total of H-bond	Ligand's atom	Amino acid residue: Atom
Rosmarinic acid	−6.72	11.79	4	O: C10=O	Gln176: H
				H: C6-OH	Val177: O
				H: C7-OH	Val177: O
				O: C6-OH	Gly179: H
Prenyl caffeate	−6.45	18.64	0	-	-
Ethyl caffeate	−5.71	65.29	7	O: C5-OH	Lys151: H
				H: C5-OH	Glu152: O
				O: C9=O	Ser180: H
				O: C9-O	Gln273: H
				H: C5-OH	Ile277: O
				H: C6-OH	Ile277: N
				H: C6-OH	Ile277: O
Methyl caffeate	−5.32	125.23	7	O: C5-OH	Lys151: H
				O: C5-OH	Glu152: H
				O: C9=O	Ser180: H
				O: C9-O	Gln273: H
				H: C5-OH	Ile277: O
				H: C6-OH	Ile277: O
				H: C6-OH	Ile277: N
Caffeoylmalic acid	−5.32	126.06	4	O: C1=O	Gln176: H
				O: C12=O	Gln176: H
				O: C12-OH	Lys 134: H
				O: C13-OH	Lys 134: H
Dihydrocaffeic acid	−5.27	136.22	4	O: C9=O	Lys151: H
				H: C5-OH	Ser180: O
				H: C6-OH	Ser180: O
				O: C5-OH	Gln273: H
Caftaric acid	−5.22	149.46	4	O: C13-OH	Lys151: H
				H: C11-OH	Val177: O
				H: C12-OH	Val177: O
				H: C11-OH	Gly179: N
Caffeic acid	−4.93	243.15	2	O: C9-OH	Lys151: H
				H: C9-OH	Ile277: O

Among the tested caffeic acid derivatives, CAPA demonstrated the most favourable binding affinity towards MexB, with a binding free energy of –7.60 kcal/mol and a predicted Ki of 2.69 M. CAPE followed closely, exhibiting a binding energy of –7.28 kcal/mol and a predicted Ki of 4.65 M. These results indicate that specific structural modifications of the phenethyl group may enhance binding affinity compared to unmodified caffeic acid.

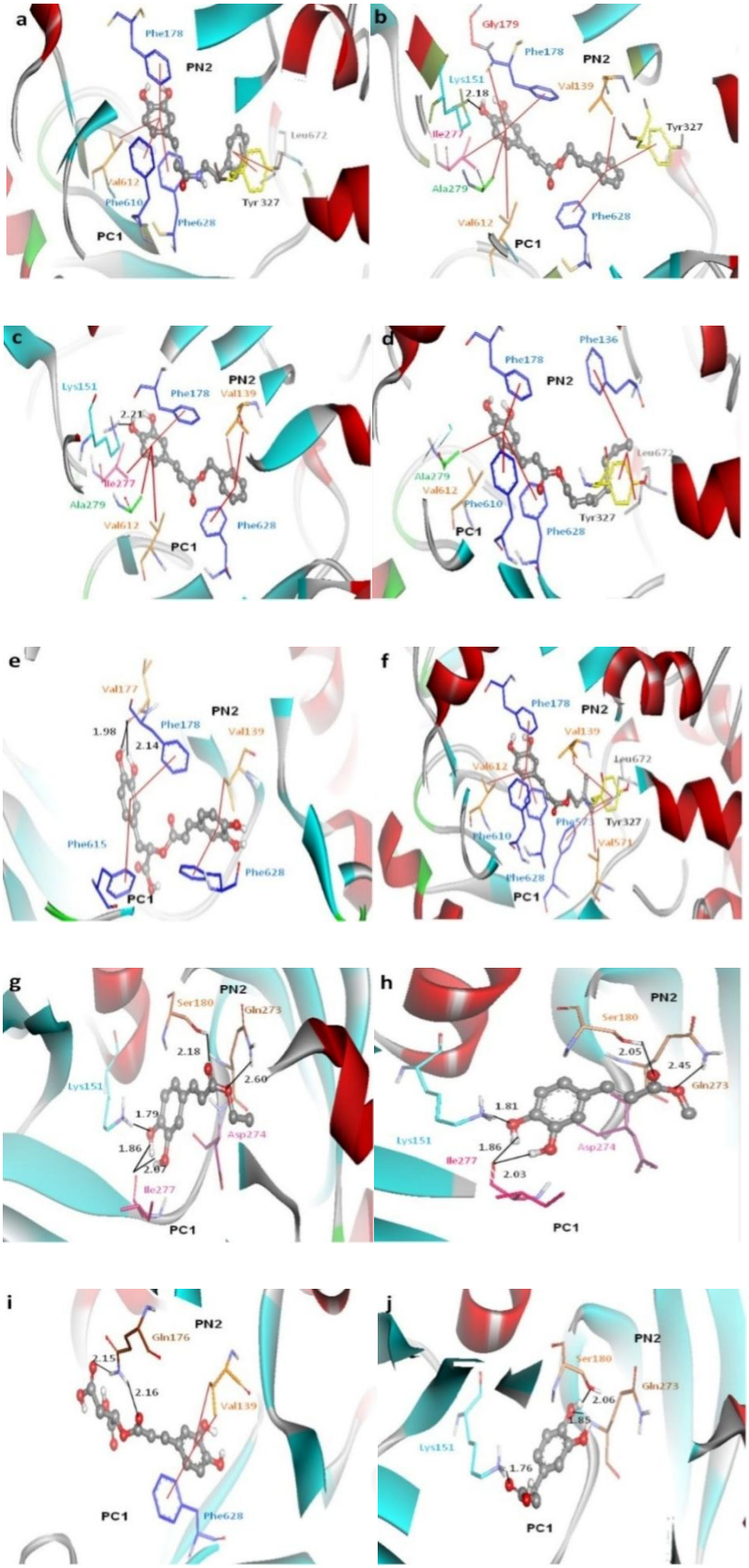
Hydrogen bonding analysis revealed varying degrees of interaction between the derivatives and the MexB protein. Ethyl caffeate and methyl caffeate formed the highest number of hydrogen bonds (n = 7), suggesting strong polar interactions with the binding site. These were followed by rosmarinic acid, caffeoylmalic acid, dihydrocaffeic acid, and caftaric acid (n = 4 each). Caffeic acid itself formed 2 hydrogen bonds, while CAPE and benzyl caffeate formed only one bond. Notably, CAPA, octyl caffeate, and prenyl caffeate did not exhibit any hydrogen bond interactions, implying that their binding may depend primarily on hydrophobic contacts or π–π stacking rather than polar interactions.

Interestingly, most of the hydrogen bonding interactions were mediated through hydroxyl and carbonyl groups on of the ligands, with Lys151 consistently emerging as a key interacting residue across several ligand complexes. This observation suggests that Lys151 may serve as a critical anchoring site within the MexB binding pocket, facilitating to ligand stabilization and binding specificity. Collectively, these findings highlight CAPA and CAPE as promising lead compounds for further development, while also underscoring the importance of both hydrophobic and polar interactions in efflux pump inhibition.

A more detailed visualization of the binding interactions between the caffeic acid derivatives and MexB was conducted using Discovery Studio Visualizer 4.1 and LigPlot+ v1.4.5, and the results are depicted in **Figures 5** and **6**, respectively. Both visualization platforms yielded consistent intermolecular interaction profiles, supporting the reliability of the observed docking poses. All docked caffeic acid derivatives, similar to the co-crystallized efflux pump inhibitor ABI-PP, were localized within the functional binding pocket of MexB, specifically near the PC1 and PN2 subdomains, which are critical for substrate recognition and transport.

The binding interactions were predominantly stabilized through a combination of hydrogen bonding and hydrophobic contacts. A key finding across several ligand complexes was the formation of hydrogen bonds with Lys151, a residue frequently involved in anchoring ligands within the binding site. However, not all caffeic acid derivatives are engaged in hydrogen bonding with this residue. For instance, CAPA, octyl caffeate, rosmarinic acid, prenyl caffeate, and caffeoylmalic acid did not exhibit hydrogen bond interactions with Lys151.

It is interesting to note that, CAPA, which exhibited the lowest binding free energy among the tested derivatives, did not form any hydrogen bonds with MexB. Instead, its binding interaction profile was dominated by extensive hydrophobic contacts involving aromatic and non-polar residues such as Phe136, Val139, Phe178, Pro326, Tyr327, Phe610, Val612, Phe628, Met630, and Leu672 (**Figures 5a** and **6a)**. This finding suggests that hydrophobic packing within the binding pocket may significantly contribute to the binding stability of CAPA-MexB complex.


a
Phe178
PN2
Leu672
Val612
Phe610
Tyr 327
Phe628
PC1
b
Gly179
Phe178
PN2
Lys151
2.18
Val139
Tyr327
Ile277
Ala279
Val612
Phe628
PC1
c
Lys151
PN2
Phe178
Val139
2.21
Ile277
Ala279
Val612
Phe628
PC1
d
Phe136
Phe178
PN2
Leu672
Ala279
Val612
Phe610
Tyr327
PC1
Phe628
e
Val177
PN2
1.98
Phe178
2.14
Val139
Phe615
Phe628
PC1
f
Phe178
PN2
Val139
Leu672
Val612
Tyr327
Phe610
Val571
Phe628
PC1
g
PN2
Ser180
Gln273
2.18
2.60
Lys151
1.79
Asp274
1.86
2.07
Ile277
PC1
h
PN2
Ser180
2.05
2.45
Gln273
1.81
Lys151
1.86
Asp274
Ile277
2.03
PC1
i
PN2
Gln176
2.15
2.16
Val139
PC1
Phe628
j
PN2
Ser180
Gln273
2.06
1.85
Lys151
1.76
PC1

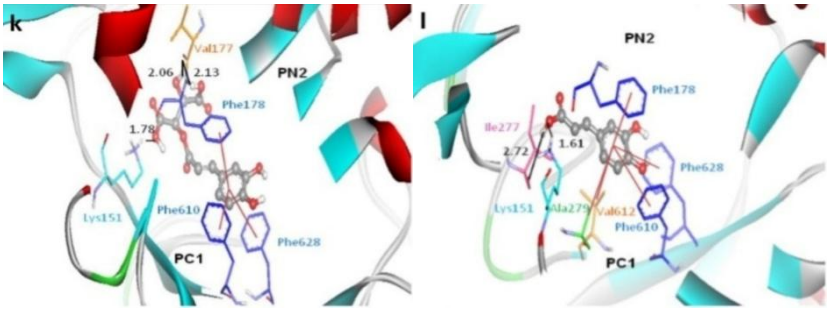
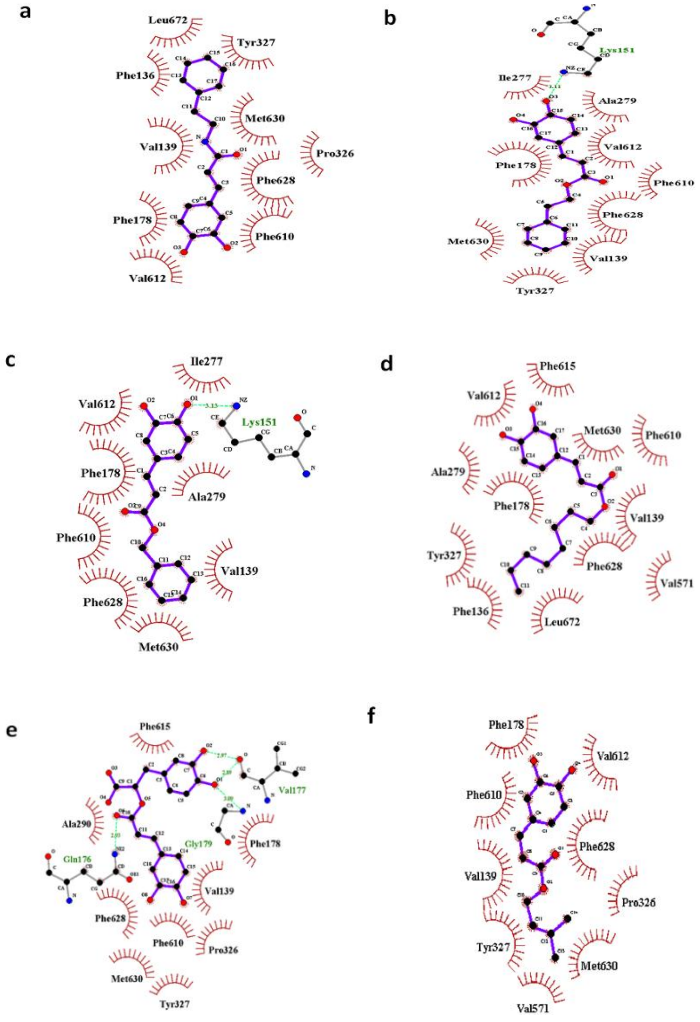


Figure 5 Three-dimensional structure of the docked caffeic acid derivatives in the MexB binding site visualized using Discovery Studio 4.1. (a) CAPA, (b) CAPE, (c) benzyl caffeate, (d) octyl caffeate, (e) rosmarinic acid, (f) prenyl caffeate, (g) ethyl caffeate, (h) methyl caffeate, (i) caffeoylmalic acid, (j) dihydrocaffeic acid, (k) caftaric acid and (l) caffeic acid. MexB is presented as ribbon and the binding site is represented as stick and colored as blue for Phe, orange (Val), green (Ala), red (Gly), magenta (Ile), yellow (Tyr), cyan (Lys), grey (Leu), plum (Asp), peach (Ser), brown (Gln) and maroon (Met). The caffeic acid derivatives are rendered as scaled ball and stick, and colored based on their atom type: grey (carbon), red (oxygen) and blue (nitrogen). Hydrogen bond and hydrophobic interactions between the caffeic acid derivatives and MexB are shown as black and red lines, respectively.



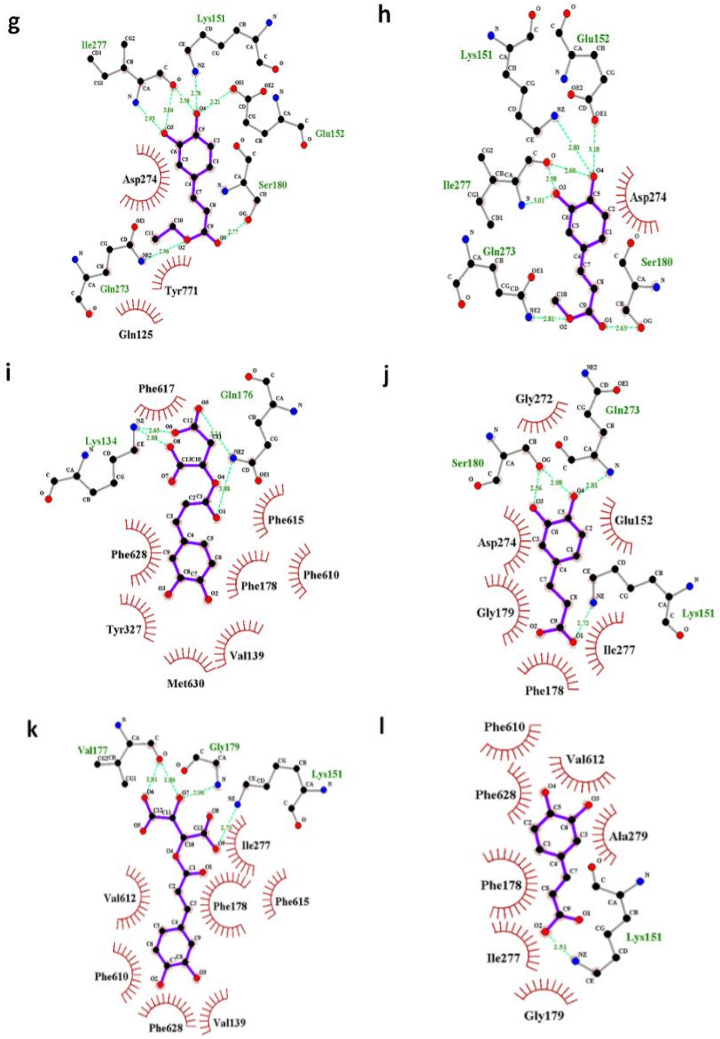


Figure 6 Two-dimensional structure of the docked caffeic acid derivatives in the MexB binding site visualized using LigPlot 1.4.5. (a) CAPA, (b) CAPE, (c) benzyl caffeate, (d) octyl caffeate, (e) rosmarinic acid, (f) prenyl caffeate, (g) ethyl caffeate, (h) methyl caffeate, (i) caffeoylmalic acid, (j) dihydrocaffeic acid, (k) caftaric acid and (l) caffeic acid. The intermolecular interactions are indicated as dashed green lines between the atoms involved for the hydrogen bonds and as arc with spokes symbols radiating towards the ligand's atom for the hydrophobic contacts.

On the other hand, CAPE, which ranked second in binding affinity, formed a single hydrogen bond between its hydroxyl group and Lys151. Additionally, CAPE engaged in multiple hydrophobic interactions with residues including Val139, Phe178, Ile277, Ala279, Tyr327, Phe610, Val612, Phe628, and Met630 (**Figures 5b** and **6b**). This dual mode of interaction (hydrogen bonding and hydrophobic contacts) likely explains for its relatively high binding affinity.

The molecular docking analysis showed that the caffeic acid derivatives preferentially bind within the distal binding pocket of MexB, particularly near the PN2 and PC1 periplasmic subdomains of the T monomer. These sites are rich in phenylalanine residues such as Phe136, Phe178, Phe610, Phe615, and Phe628, which facilitate strong π–π stacking and hydrophobic interactions with the docked ligands. This binding pattern resembles that of the known efflux pump inhibitor ABI-PP, whose activity is similarly stabilized by interactions with key phenylalanine residues, especially Phe178 [43].

Interestingly, the predicted docking site of the caffeic acid derivatives corresponded closely to the binding region of several well-characterized ligands of resistance-nodulation-division (RND) transporters. This includes meropenem, which has been co-crystallized

within the distal binding pocket of MexB protein, and the binding site of the established EPI, phe-arg-β-naphthylamide (PAβN) in the AcrB protein, a homologous of MexB, [30,53]. In addition, the binding site of the docked poses of caffeic acid derivatives also aligned well with the binding site of the detergent dodecylmaltoside, as well as the binding site of an antibiotic minocycline and drug doxorubicin, the 2 bulky scaffolds with aromatic-rich molecules that previously co-crystallized to the MexB and AcrB proteins, respectively [43,55]. These comparison compounds are generally characterized by their bulky structures and abundance of aromatic systems as well as hydrophobic moieties, characteristics that appear similarly important for the favorable docking observed for the caffeic acid derivatives. Taken together, the overlap of binding locations across these structurally diverse yet functionally validated ligands support the interpretation that the distal binding pocket of MexB protein is an important key site for drug binding and a promising target for efflux pump inhibition. Bulky compounds that contain aromatic rings and other hydrophobic groups in this study like ABI-PP would have better interaction with MexB protein [53, 55]. This also helps justify why compounds such as ABI-PP and the caffeic acid derivatives demonstrate stable interactions with the MexB binding cavity. Including these comparator ligands also allows us to frame our docking findings in the context of experimentally supported structural biology data, thereby increasing the robustness and interpretive confidence of the docking predictions.

Among the tested derivatives, CAPE and CAPA exhibited the most favorable docking scores, indicating stronger interactions with the MexB. Their enhanced binding affinity is likely attributed to the presence of aromatic hydrocarbon rings and ethyl moieties, which contribute to hydrophobic interactions and π–π stacking within the MexB binding pocket. Although their predicted binding energies were higher than that of the reference efflux pump inhibitor ABI-PP, both CAPE and CAPA displayed comparable binding orientations and interactions with key residues implicated in substrate recognition, suggesting that they may exert efflux inhibition through similar mechanisms. It should be noted, however, that the present findings are based solely on molecular docking and therefore represent a preliminary, hypothesis-generating assessment of efflux pump inhibition. Further validation using molecular dynamics simulations combined with binding free energy calculations (e.g., MM/PBSA) would be valuable to assess the stability and dynamics of the CAPA-MexB and CAPE–MexB complexes over time. Experimental validation through efflux inhibition assays or antibiotic synergy studies would be also essential to substantiate the computational predictions and establish their functional relevance.

Conclusions

To summarize, the above findings highlight the potential of caffeic acid derivatives, especially CAPE and CAPA as novel efflux pump inhibitor (EPI) scaffolds. The presence of both hydrophilic (e.g., phenol and amide groups) and hydrophobic features in CAPE and CAPA contributes to their amphiphilic character, a structural property frequently recognized by multidrug efflux pumps. Their favorable binding affinity, structural compatibility with the MexB binding pocket, and shared pharmacophore features with known inhibitors highlight their potential as promising scaffolds for the development of novel EPIs.

These findings have broader implications for combating multidrug resistance in *Pseudomonas aeruginosa*, as the inhibition of efflux pumps has the potential to restore antibiotic efficacy and enhance the effectiveness of existing antimicrobial therapies. By identifying CAPE and CAPA as promising scaffolds, this study contributes to ongoing efforts to develop adjuvant therapies aimed at mitigating the clinical impact of resistant *P. aeruginosa* infections. However, the present study is limited to *in silico* analyses, which do not fully capture the dynamic behavior of ligand binding or the complex physiological context in which efflux pumps operate. Future studies should incorporate molecular dynamics simulations to assess the stability and conformational behavior of the CAPE–MexB and CAPA–MexB complexes, as well as SAR-based optimization to improve potency and specificity. Experimental validation such as efflux inhibition assays, antibiotic synergy testing, and microbiological evaluation would be essential to substantiate these computational predictions and determine their translational potential. Collectively, these efforts would provide a more comprehensive understanding of the

therapeutic potential of CAPE and CAPA as efflux pump inhibitors.

Acknowledgements

The authors would like to thank the Universiti Sains Malaysia (USM), Pulau Pinang, Malaysia for providing financial assistance through the Research University (RU) grant (1001/PFARMASI/811237).

Declaration of generative AI in scientific writing

The authors declare that no generative artificial intelligence (AI) tools were used during the preparation of this manuscript. All authors have reviewed and approved the final version and assume full responsibility for the content and conclusions of this work.

CRediT author statement

Noor Zawani Zakaria: Conceptualization, Methodology, Literature search, Data curation, Validation, Writing -original draft. **Habibah A Wahab:** Conceptualization, Methodology, Validation. **Suriani Mohamad:** Conceptualization, Methodology, Literature search, Data curation, Validation, Writing original draft, Writing -review & editing, Project administration, Supervision. **Ezatul Ezleen Kamarulzaman:** Conceptualization, Methodology, Literature search, Data curation, Validation, Visualization, Writing -review & editing, Project administration, Supervision.

References

[1] I Jurado-Martin, M Sainz-Mejias and S McClean. *Pseudomonas aeruginosa*: An audacious pathogen with an adaptable arsenal of virulence factors. *International Journal of Molecular Sciences* 2021; **22(6)**, 3128.

[2] M Haque, M Sartelli, J McKimm and M Abu Bakar. Health care-associated infections - an overview. *Infection and Drug Resistance* 2018; **11**, 2321-2333.

[3] KL McCarthy and DL Paterson. Increased risk of death with recurrent *Pseudomonas aeruginosa* bacteremia. *Diagnostic Microbiology and Infectious Disease* 2017; **88(2)**, 152-157.

[4] MD Parkins, R Somayaji and VJ Waters. Epidemiology, biology, and impact of clonal *Pseudomonas aeruginosa* infections in cystic fibrosis. *Clinical Microbiology Reviews* 2018; **31(4)**, e00019-18.

[5] XZ Li, P Plesiat and H Nikaido. The challenge of efflux-mediated antibiotic resistance in Gram-negative bacteria. *Clinical Microbiology Reviews* 2015; **28(2)**, 337-418.

[6] J Dreier and P Ruggerone. Interaction of antibacterial compounds with RND efflux pumps in *Pseudomonas aeruginosa*. *Frontiers in Microbiology* 2015; **6**, 660.

[7] S Guenard, C Muller, L Monlezun, P Benas, I Broutin, K Jeannot and P Plesiat. Multiple mutations lead to MexXY-OprM-dependent aminoglycoside resistance in clinical strains of *Pseudomonas aeruginosa*. *Antimicro-bial Agents and Chemotherapy* 2014; **58**, 221-228.

[8] MB Habib, NA Shah, A Amir, HA Alghamdi, MH Tariq, K Nisa and M Ammoun. Decoding MexB efflux pump genes: structural, molecular, and phylogenetic analysis of multidrug-resistant and extensively drug-resistant *Pseudomonas aeruginosa*. *Frontiers in Cellular and Infection Microbiology* 2025; **14**, 1519737.

[9] E Kello, R Greenberg, W Li, S Polansky, R Maldonado, Y Peter and P Basu. The effect of antibiotic treatment and gene expression of Mex B efflux transporters on the resistance in *Pseudomonas aeruginosa* biofilms. *Applied Microbiology* 2023; **3(3)**, 709-721.

[10] M Duffey, RP Jumde, RMA da Costa, HK Ropponen, B Blasco and LJV Piddock. Extending the potency and lifespan of antibiotic: Inhibitors of Gram-negative bacterial efflux pumps. *ACS Infectious Diseases* 2024; **10(5)** 1458-1482.

[11] RP Lamers, JF Cavallari and LL Burrows. The efflux inhibitor phenylalanine-arginine beta-naphthylamide (PAβN) permeabilizes the outer membrane of Gram-negative bacteria. *PLoS One* 2013; **8(3)**, e60666.

[12] S Schuster, JA Bohnert, M Vavra, JW Rossen and WV Kern. Proof of an outer membrane target of the efflux inhibitor Phe-Arg-β-Naphthylamide from random mutagenesis. *Molecules* 2019; **24(3)**, 470.

[13] AD Kinana, AV Vargiu, T May and H Nikaido. Aminoacyl β-Naphthylamides as substrates and modulators of AcrB multidrug efflux pump.

Proceedings of the National Academy of Sciences of the United States of America 2016; **113(5),** 1405-1410.

[14] N Bamola, P Verma and C Negi. A review on some traditional medicinal plants. *International Journal of Life Sciences Scientific Research* 2018; **4(1)** 1550-1556.

[15] M Dev and M Mukadam. Functional group profiling of medicinal plants using FTIR spectroscopy. *World Journal of Biology Pharmacy and Health Sciences* 2025, **21(01),** 243-249.

[16] MN Clifford. Chlorogenic acids and other cinnamates - nature, occurrence, dietary burden, absorption and metabolism. *Journal of the Science of Food and Agriculture* 2000; **80**, 1033-1043.

[17] C Chaowuttikul, C Palanuvej and N Ruangrungsi. Quantification of chlorogenic acid, rosmarinic acid, and caffeic acid contents in selected Thai medicinal plants using RP-HPLC-DAD. *Brazilian Journal of Pharmaceutical Sciences* 2020; **56**, e17547.

[18] F Khan, NI Bamunuarachchi, N Tabassum and YM Kim. Caffeic acid and its derivatives: Antimicrobial drugs toward. *Microbial Pathogens Journal of Agricultural and Food Chemistry* 2021; **69(10)**, 2979-3004.

[19] NN Muhammad Abdul Kadar, F Ahmad, SL Teoh and MF Yahaya. Caffeic acid on metabolic syndrome: A review. *Molecules* 2021; **26(18)**, 5490.

[20] N Pavlikova. Caffeic acid and diseases-mechanisms of action. *International Journal of Molecular Sciences* 2022; **24(1)**, 588.

[21] H Wang, GJ Provan and K Helliwell. Determination of rosmarinic acid and caffeic acid in aromatic herbs by HPLC. *Food Chemistry* 2004; **87(2)**, 307-311.

[22] RW Jiang, KM Lau, PM Hon, TC Mak, KS Woo and KP Fung. Chemistry and biological activities of caffeic acid derivatives from *Salvia miltiorrhiza*. *Current Medicinal Chemistry* 2005; **12(2)**, 237-246.

[23] M Yoshimoto, R Kurata-Azuma, M Fujii, H De-Xing, K Ikeda, T Yoshidome and M Osako. Enzymatic production of caffeic acid by Koji from plant resources containing caffeoylquinic acid derivatives. *Bioscience, Biotechnology, and Biochemistry* 2005; **69(9)**, 1777-1781.

[24] J Yu, J Xie, M Sun, S Xiong, C Xu, Z Zhang, M Li, C Li and L Lin. Plant-derived caffeic acid and its derivatives: An overview of their NMR data and biosynthetic pathways. *Molecules* 2024; **29(7)**, 1625.

[25] A Trivedi, S Bhati and A Joshi. Establishment of callus cultures and quantification of caffeic acid using HPTLC from *Desmodium gangeticum* (L.). *Natural Product Research* 2025; **39(17)**, 4871-4878.

[26] P Dhiman, N Malik and A Khatkar. Hybrid caffeic acid derivatives as monoamine oxidases inhibitors: Synthesis, radical scavenging activity, molecular docking studies and *in silico* ADMET analysis. *Chemistry Central Journal* 2018; **12**, 112.

[27] K Sidoryk, A Jaromin, N Filipczak N, P Cmoch and M Cybulski. Synthesis and antioxidant activity of caffeic acid derivatives. *Molecules* 2018; **23(9)**, 2199.

[28] MD Armas-Ricard, E Ruiz-Reyes and O Ramírez-Rodríguez. Caffeates and caffeamides: Synthetic methodologies and their Antioxidant properties. *Hindawi International Journal of Medicinal Chemistry* 2019; **2019**, 2592609.

[29] X Peng, G Wu, A Zhao, K Huang, L Chai, B Natarajan, S Yang, H Chen and C Lin. Synthesis of novel caffeic acid derivatives and their protective effect against hydrogen peroxide induced oxidative stress via Nrf2 pathway. *Life Sciences* 2020; **247**, 117439.

[30] Y Mou, S Wen, HK Sha, Y Zhao, LJ Gui, Y Wang and ZY Jiang. Discovery and development of caffeic acid analogs as versatile therapeutic agents. *Pharmaceuticals* 2024; **17(10)**, 1403.

[31] X Zhao, ZW Liu, H Liu, J Guo and SH Long. Hybrid molecules based on caffeic acid as potential therapeutics: A focused review. *European Journal of Medicinal Chemistry* 2022; **243**, 114745.

[32] K Sakae, D Nonaka, M Y Hirata, R Fujiwara, A Kondo, S Noda and T Tanaka. Caffeic acid production from glucose using metabolically engineered *Escherichia coli*. *Enzyme and Microbial Technology* 2023; **164**, 110193.

[33] H Shen, A Yamashita, M Nakakoshi, H Yokoe, M Sudo, H Kasai, T Tanaka, Y Fujimoto, M Ikeda, N Kato, N Sakamoto, H Shindo, S Maekawa and K Moriishi. Inhibitory effects of caffeic acid phenethyl ester derivatives on replication of hepatitis C virus. *PLOS One* 2013; **8(12)**, e82299.

[34] H Utsunomiya, M Ichinose, K Ikeda, M Uozaki, J Morishita, T Kuwahara, AH Koyama and H Yamasaki. Inhibition by caffeic acid of the influenza A virus multiplication *in vitro*. *International Journal of Molecular Medicine* 2014; **34**, 1020-1024.

[35] JCO Sardi, FP Gullo, IA Freires, NS Pitangui, MP Segalla, AM Fusco-Almeida, PL Rosalen, LO Regasini and MJS Mendes-Giannini. Synthesis, antifungal activity of caffeic acid derivative esters, and their synergism with fluconazole and nystatin against *Candida* spp. *Diagnostic Microbiology and Infectious Disease* 2016; **86(4)**, 387-391.

[36] M Kepa, M Miklasinska-Majdanik, RD Wojtyczka, D Idzik, K Korzeniowski, J Smolen-Dzirba and TJ Wasik. Antimicrobial potential of caffeic acid against *Staphylococcus aureus* clinical strains. *Biomedical Research International* 2018; **15**, 7413504.

[37] FCP Rossatto, N Tharmalingam, IE Escobar, PA d'Azevedo, KR Zimmer and E Mylonakis. Antifungal Activity of the phenolic compounds Ellagic Acid (EA) and Caffeic Acid Phenethyl Ester (CAPE) against Drug-Resistant *Candida auris*. *Journal of Fungi* 2021; **7(9)**, 763.

[38] W Sun and MH Shahrajabian. Therapeutic potential of phenolic compounds in medicinal plants - Natural health products for human health. *Molecules* 2023; **28(4)**, 1845.

[39] M Bhattacharya and S Mandal. Antibacterial activity of caffeic acid from plant sources: A review based on *in silico, in vitro* and *in vivo* approaches. *The Microbe* 2025; **8**, 100541.

[40] M Salehi, I Haghani, M Saeedi, K Morteza-Semnani, R Negarandeh, A Hosseinnataj, A Jafari, A Lotfizadeh, A Rafiei and T Molania. Antifungal efficacy of caffeic acid and nano-caffeic acid particles against candidiasis: An *in vitro* study. *Journal of Oral Microbiology* 2025; **17(1)**, 2564690.

[41] MV Saivish, CC Pacca, VG da Costa, GL Menezes, RA da Silva, L Nebo, GSD da Silva, BRGA Milhim, IS Teixeira, T Henrique, NFB Mistrão, VM Hernandes, N Zini, AC de Carvalho, MA Fontoura, P Rahal, L Sacchetto, RE Marques and ML Nogueira. Caffeic acid has antiviral activity against Ilhéus virus *in vitro*. *Viruses* 2023; **15(2)**, 494.

[42] GM Morris, R Huey, W Lindstrom, MF Sanner, RK Belew, DS Goodsell and J Olson. AutoDock4 and AutoDockTools4: Automated docking with selective receptor flexibility. *Journal of Computational Chemistry* 2009; **30(16)**, 2785-2791.

[43] R Nakashima, K Sakurai, S Yamasaki, K Hayashi, C Nagata, K Hoshino, Y Onodera, K Nishino and A Yamaguchi. Structural basis for the inhibition of bacterial multidrug exporters. *Nature* 2013; **500**, 102-106.

[44] C Lipinski, F Lombardo, BW Dominy and PJ Feeney. Experimental and computational approaches to estimate solubility and permeability in drug discovery and development settings. *Advanced Drug Delivery Reviews* 1997; **23**, 3-25.

[45] S Forli, R Huey, ME Pique, MF Sanner, DS Goodsell and AJ Olson. Computational protein-ligand docking and virtual drug screening with the Autodock suite. *Nature Protocols* 2016; **11**, 905-919.

[46] FJ Solis and RJB Wets. Minimization by random search techniques. *Mathematics of Operations Research* 1981; **6(1)**, 19-30.

[47] GM Morris, DS Goodsell, RS Halliday, R Huey, WE Hart, RK Belew and AJ Olson. Automated docking using a Lamarckian genetic algorithm and an empirical binding free energy function. *Journal of Computational Chemistry* 1998; **19(14)**, 1639-1662.

[48] RA Laskowski and MB Swindells. Ligplot+: Multiple ligand-protein interaction diagrams for drug discovery. *Journal of Chemical Information and Modeling* 2011; **51(10)**, 2778-2786.

[49] J Fu, K Cheng, ZM Zhang, RQ Fang and HL Zhu. Synthesis, structure and structure-activity relationship analysis of caffeic acid amides as potential antimicrobials. *European Journal of Medicinal Chemistry* 2010; **45(6)**, 2638-2643.

[50] RP Verma and C Hansch. An approach towards the quantitative structure-activity relationships of caffeic acid and its derivatives. *ChemBioChem* 2004; **5(9)**, 1188-1195.

[51] M Touaibia, J Jean-Francoise and J Doiron. Caffeic acid, a versatile pharmacophore: An overview. *Mini-Reviews in Medicinal Chemistry* 2011; **11(8)**, 695-713.

[52] J Yang, GA Marriner, X Wang, PD Bowman, SM Kerwin and S Stavchansky. Synthesis of a series of caffeic acid phenethyl amide (CAPA) fluorinated derivatives: Comparison of cytoprotective effects to caffeic acid phenethyl ester (CAPE). *Bioorganic and Medicinal Chemistry* 2010; **18(14)**, 5032-5038.

[53] EW Yu, G McDermott, HI Zgurskaya, H Nikaido and DE Koshland. Structural basis of multiple drug-binding capacity of the AcrB multidrug efflux pump. *Science* 2003; **300(5621)**, 976-980.

[54] D Seeliger and BL de Groot. Conformational transitions upon ligand binding: Holo-structure prediction from apo conformations. *Biophysical Journal* 2010; **98(3)**, 428a.

[55] F Collu, AV Vargui, J Dreier, M Casella and P Ruggerone. Recognition of imipenem and meropenem by RND-transporter MexB studied by computer simulations. *Journal of the American Chemical Society* 2012; **134(46)**, 19146-19158.